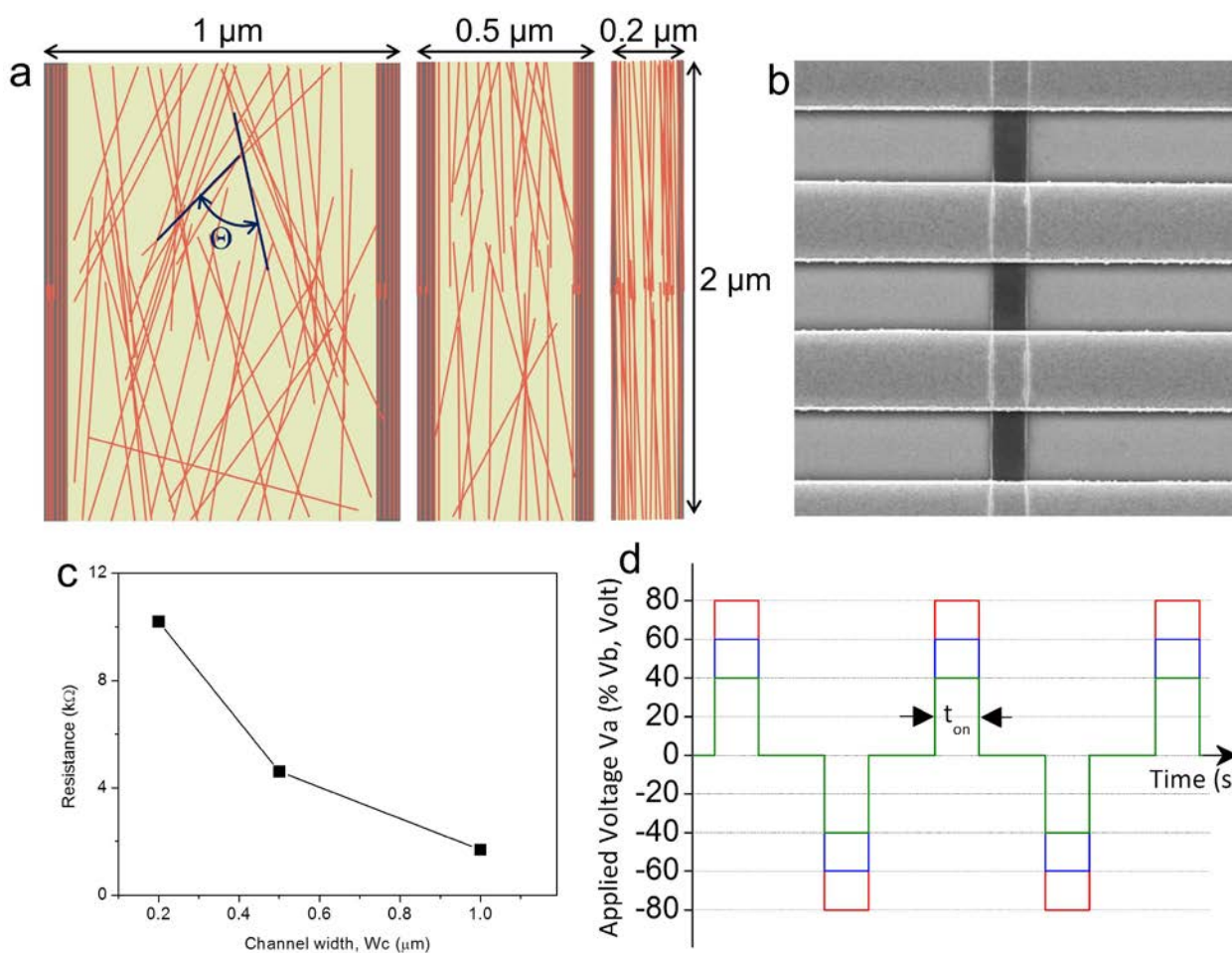# Supplement information
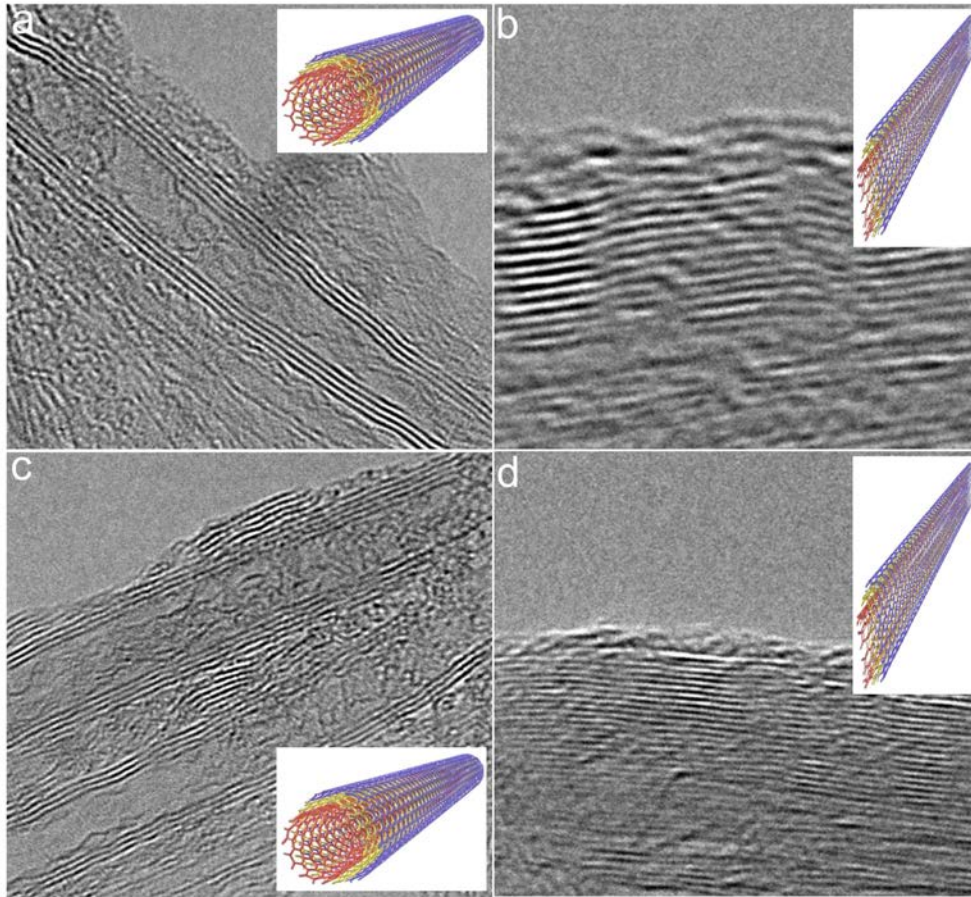
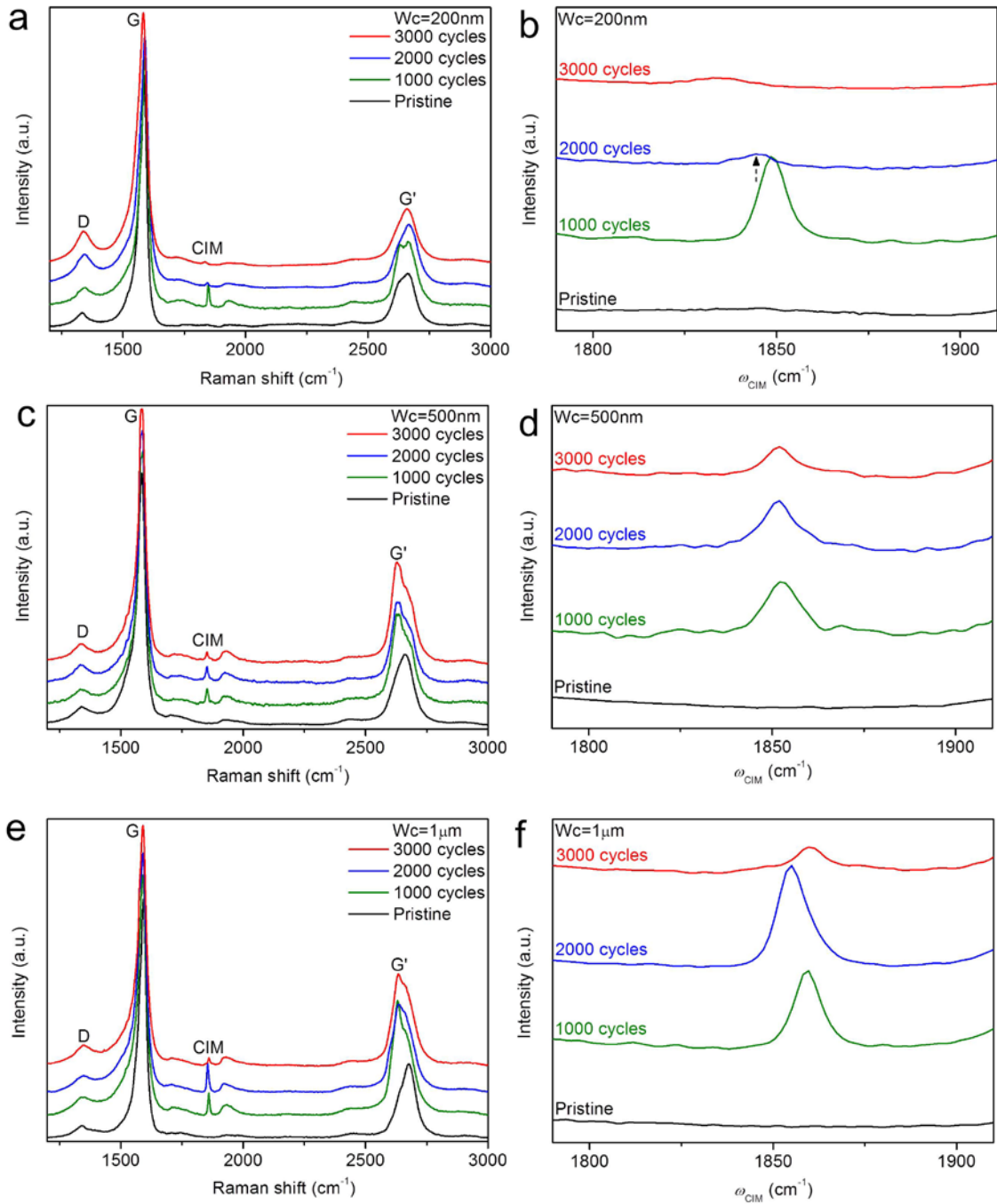**Supplement figures**
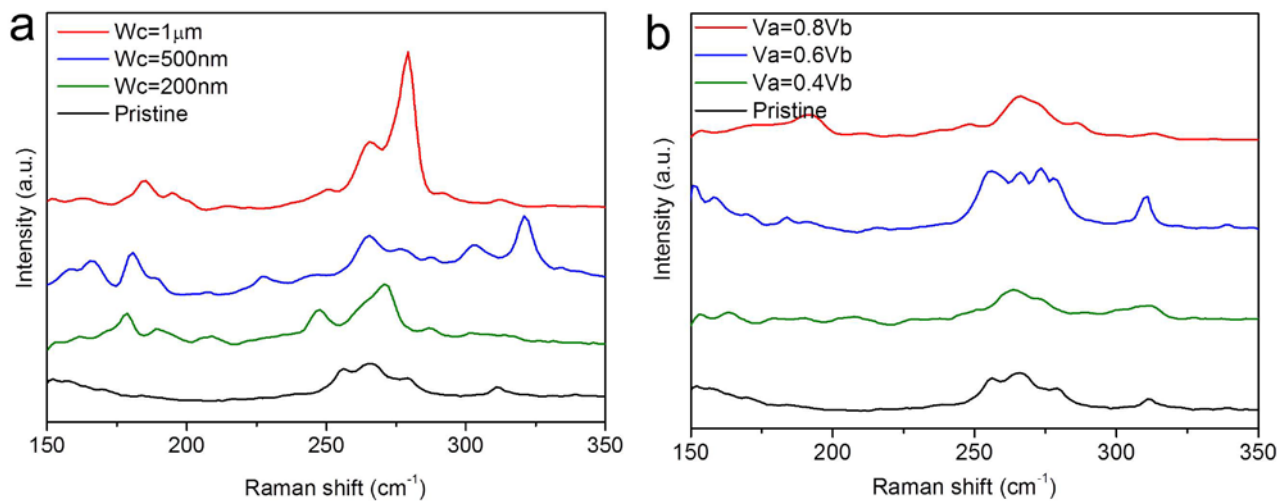

Supplementary Figure S1 │ Illustration of SWCNT networks in W_c=1, 0.5 and 0.2 μm channel width, SEM, Resistance of the networks, and time-dependent alternating voltage pulses (a) the illustration of aligned carbon nanotube structures in the networks with varying channel width, W_c=1, 0.5 and 0.2 μm, which is extracted from the SEM images in the Figure 1. Θ indicates the inter-tubes alignment angles (b) SEM image of an assembled SWCNT network (W_c=1 μm) integrated with electrodes. The interval distance of two electrodes is 2 μm. (c) Effect of channel width on the resistance of the assembled SWCNT networks. (d) The overall transformation process by applied voltage pulse at 80, 60 and 40% of breakdown voltages. The t_{on} indicates source duration time, where t_{on}=0.1s.
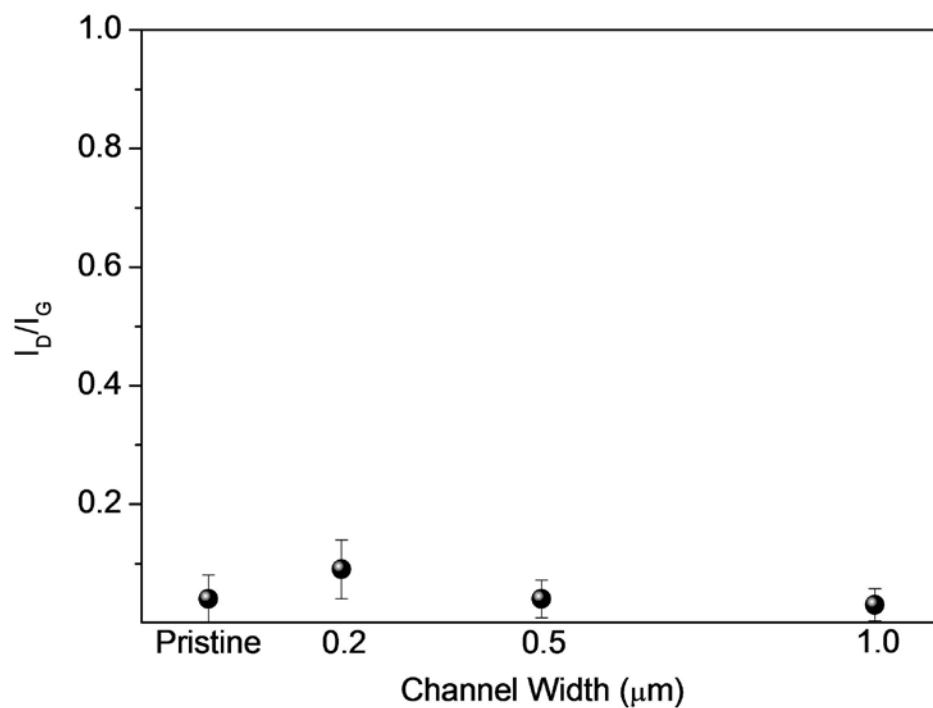
Supplementary Figure S2 │ TEM images of transformed carbon structures. (a) MWCNTs and (b) MGNRs are obtained by treating electrically at (a) 0.6Vb and (b) 0.8Vb voltage condition using the W_c=0.5 μm network. (c) MWCNTs and (d) MGNRs are obtained by treating electrically at (c) 0.6Vb and (d) 0.8Vb voltage condition using the W_c=1 μm network.

Supplementary Figure S3 │ Resonant Raman spectra of the SWCNT network with W_c=0.2, 0.5 and 1 μm channel width as function of cycles. The RRS of the SWCNT networks for W_c=0.2 μm (a-b), 0.5 μm (c-d) and 1 μm (e-f), where the applied voltage is $0.8V_b$ and the number of cycles are 1000, 2000, and 3000 cycles. The CIM frequency range of (b,d,f) are zoomed from (a,c,e), respectively. The peak intensity of the CIM, I_{CIM} continues to grow with increasing voltage cycling until reaching the maximum peak, and then the structural transformation rate gradually slows down.

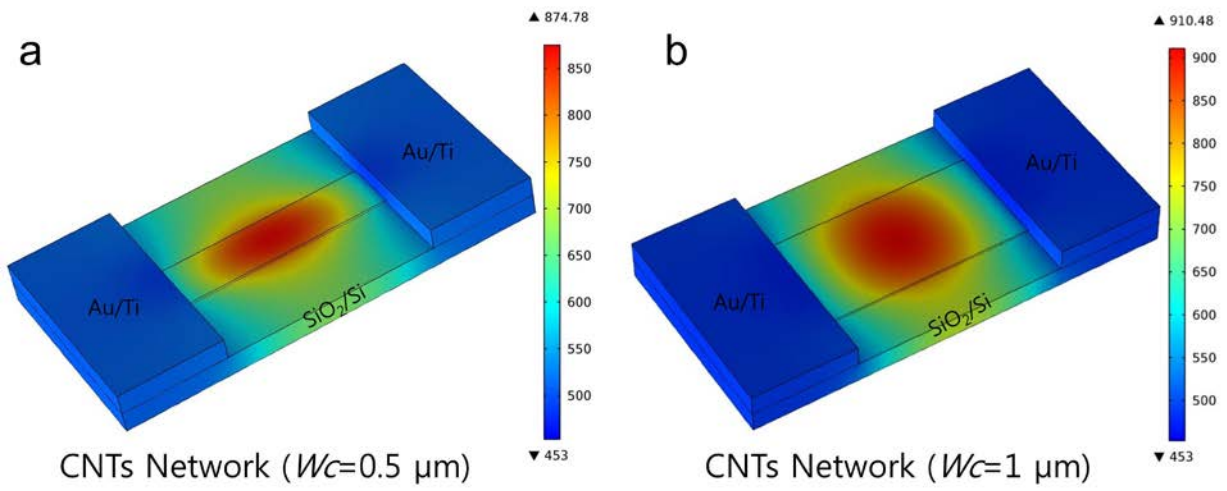**Supplementary Figure S4 │ RBMs spectra.** The spectra were measured with a 532 nm (2.33 eV) laser line. (a) The peaks were compared with the RBMs as function of channel width for Wc=0.2, 0.5 and 1μm extracted from the Fig. 2a. (b) The RBM peaks for Wc=0.2 μm channel width were compared as function of applied voltage pulses between $0.4V_b$ to $0.8V_b$ extracted from the Fig. 3a.

Supplementary Figure S5 │ Comparison of D and G intensity ratio. The ratio of the D and G band (I_D/I_G) as a function of channel width for Wc=0.2, 0.5 and 1μm were obtained from Raman spectroscopy before and at the end of 2000 cycles. This ratio is a measure of disorder density in SWCNTs, which is found to decrease as channel width is increased. Error bars represent the s.d.

Supplementary Figure S6 │ Real-time resistance. The in-situ resistance changes for the (a) W_c=0.5 μm and (b) 1 μm array as a function of the number of cycles at V_a=0.4V_b, 0.6V_b and 0.8V_b voltage conditions. (c) The post-cycling electrical resistance change to pristine resistance as a function of channel widths and applied voltages.

Supplementary Figure S7 │ Simulated temperature profile. The temperature profile by the 3D COMSOL multiphysics of the SWCNT networks at V_a=0.8V_b voltage condition. (a) The maximum temperature of W_c=0.5 μm network is around 850 K. (b) The maximum temperature of W_c=1 μm network is around 910 K.

Supplementary Notes

Raman measurements: The RBMs (first-order Raman process) are phonon modes in which the carbon atoms along the CNT circumference are vibrating in phase, so that the nanotubes, when in resonance to these modes, behave as if they were breathing[1-3]. A remarkable feature behind the RBMs is that they are inversely proportional to the CNT diameter (d_t) so that each particular CNT vibrates at its very own RBM frequency (ω_{RBM})[1-5]. This makes the observation of changes in the RBM region important to strength any hypothesis of structural changes in any CNTs[5]. To strengthen our interpretation of the Raman spectra, we followed the RBM intensity profile changes for each device. In supplementary Fig. S4, the spectra were measured with a 532 nm (2.33 eV) laser line. The peaks in the supplementary Fig. S4a were compared with the RBMs as function of channel width for Wc=0.2, 0.5 and 1μm extracted from the Fig. 2a. The RBM peaks for Wc=0.2 μm channel width in the supplementary Fig. S4b were compared as function of applied voltage pulses between $0.4V_b$ to $0.8V_b$ extracted from the Fig. 3a. Since the relative RBM intensities reflect the amount of each CNT species observed in the sample, one can see that most of the time we have more changes in the amount of nanotubes with small d_t (referring to the region with RBM frequencies bigger than 170 cm^{-1}) than changes in the amount of CNTs with large dt (referring to the region with RBM frequencies smaller than 170 cm^{-1}). This is also consistent with the fact that small diameter tubes will be affected first, before tubes with large diameters[1-5].

This hypothesis is also confirmed and manifested in the G'-band spectra in Fig. 3c. As described by Sousa-filho *et al.*[6], the G'-band in CNTs structures are directly connected to their diameters. This means that the G'-band must change its lineshape and intensity profile if the diameter distributions changes. As shown in Fig. 3c, in fact the G'-band spectra changes when departing from the pristine sample to the $0.8V_b$ voltage case. It is noteworthy that the region referent to small diameter tubes (around 2622 cm^{-1} as highlighted in Fig. 3c) changes more the region referent to large diameters (around 2666 cm^{-1}) which confirms our interpretations. This is consistent with the coalescence of SWCNTs, which form MWCNTs, and the collapse of MWCNTs into their layer-stacked MGNR

counterparts.

To further enforce the random network self-organization hypothesis, we addressed in the supplementary Fig. S5 the ratio I_D/I_G as a function of channel width for Wc=0.2, 0.5 and 1μm extracted from the Fig. 2a. The result show that I_D/I_G after the transformation process decrease with increasing channel width what means that the network is getting less defective and more organized to form essentially sp^2 carbon materials.

Supplementary References

1. Saito, et al. *Advances in Physics* 2011*, **60**, 413.

2. A. Jorio, M. S. Dresselhaus, R. Saito and G. Dresselhaus, Wiley-VCH Verlag GmbH & Co KGaA, WeinHeim, Germany, 2011.

3. Pimenta, et al. *Phys. Chem. Chem. Phys.* 2007, **9**, 1276.

4. M. S. Dresselhaus, G. Dresselhaus, R. Saito and A. Jorio, *Phys. Rep.* 2005, **409**, 47.

5. H. Y. Jung, P. T. Araujo, Y. L. Kim. S. M. Jung, X. Jia, S. Hong, C. W. Ahn, J. Kong, M. S. Dresselhaus, S. Kar and Y. J. Jung, *Nat. Commun.,* 2014, **5**:4941 doi:10.1038/ncomms5941.

6. A. G. Souza Filho, A. Jorio, G. Samsonidze, G. Dresselhaus, M. A. Pimenta, M. S. Dresselhaus, A. K. Swan, M. S. Unlu, B. B .Goldberg and R. Saito, *Phys. Rev. B* 2003, **67**, 035427.